2.10 Vector Network Analyzers (VNAs)

S-parameters are such a fundamental part of RF and microwave analysis and design that it is important to have a simple but accurate way of measuring them. The vector network analyzer (VNA) is an instrument that is capable of making such measurements quickly (most often for two-port networks, but analyzers capable of handling more than two ports are available). A VNA can measure complex quantities in the frequency domain (analyzers that can measure only magnitudes are called scalar network analyzers or SNAs), and so can determine not only reflection and transmission coefficients but also impedances and admittances. Using the Fast Fourier Transform (FFT), the time domain response of microwave networks can be measured as well. The VNA is a part of every modern microwave lab. Major manufacturers of VNAs are Agilent (formerly Hewlett-Packard), Anritsu and Rohde & Schwarz. The most sophisticated network analyzer on the market today is the Agilent ENA and PNA network analyzer series (which have replaced the classic HP 8510C VNA). The 65-GHz version costs around $240,000, while the 110-GHz precision network analyzer costs in the neighborhood of $500,000 (2005 data). There are ways to do measurements up to 650 GHz, and the price goes up accordingly. The reason is that microwave components at higher frequencies are much harder to make with low losses, and for active devices, obtaining enough power from semiconductor devices is a problem.

We will present a more detailed description of the operation of a VNA in sections 4.5-4.6 of chapter 4, but we wish here to focus only on a very important aspect of VNA operation—its *calibration*. A real, two-port VNA can be represented as an ideal (error-free) two-port VNA to which an "error box" has been connected at each port, and one between the ports, as shown in Fig. 2.15. Of course, this is

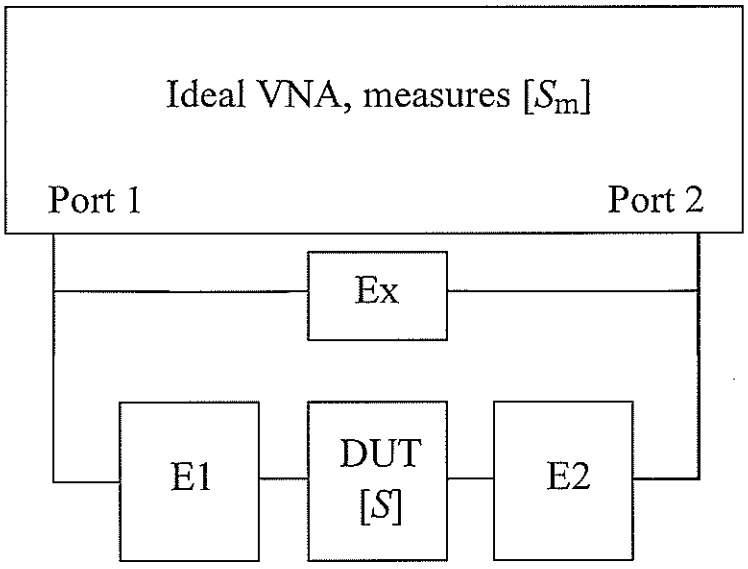

Figure 2.15: Model of a two-port VNA as an ideal VNA with an error box at each port connected to the device under test (DUT), and an error box between port 1 and port 2.

not what the VNA actually looks like inside, but it is an equivalent circuit for it in the same spirit as a Thévenin equivalent circuit is for an ordinary two-terminal network. The ideal VNA measures not the S-parameters of the device under test (DUT), but the parameters $[S_m]$ of the composite two-port formed by cascading error box E1 with the DUT and the second error box E2, and the result connected in parallel with an error box Ex representing imperfect isolation effects (leakage between ports 1 and 2) that are important in transmission calibration.

The error boxes account for the many ways in which inaccuracies may enter into the "raw" measured S-parameters $[S_m]$: the effect of the test port cables and coaxial connectors, tolerances on components used in the VNA circuits, variations caused by changes in temperature, pressure, humidity, etc. At lower frequencies, the errors of measurement instruments such as multimeters are generally small and can be compensated for on a long term basis (over a number of years), but at microwave frequencies their effect is more serious, and we must perform a calibration of the VNA before every use in order to determine the S-parameters of the error boxes and remove their influence on the raw measured data.

Calibration is accomplished by connecting known (or at least partially known) devices known as *calibration standards* (or *cal standards* for short) to the measurement ports of the VNA, and using the measured raw S-parameters to deduce information about the error boxes. Once we have this information, we can measure unknown DUTs on the VNA, which will use an internal microprocessor to eliminate the effect of the error boxes from the raw data and display the actual S-parameters of the DUT. As an example, if a one-port termination whose reflection coefficient is S_{11} is attached to port 1, the raw reflection coefficient measured at the ideal VNA can be shown to be

$$S_{m11} = r_{1d} + t_1^2 \frac{S_{11}}{1 - r_{1s} S_{11}} \tag{2.30}$$

where the $[S]$ matrix of error box E1 (assumed to be reciprocal) is given by

$$[S_{E1}] = \begin{bmatrix} r_{1d} & t_1 \\ t_1 & r_{1s} \end{bmatrix} \tag{2.31}$$

In the following subsections we will indicate two ways of finding the S-parameters of the error boxes using measurements of cal standards. Once the elements of $[S_{E1}]$ have been found, we can determine S_{11} from the "raw" or "uncalibrated" measured value S_{m11} as:

$$S_{11} = \frac{S_{m11} - r_{1d}}{t_1^2 + r_{1s}\left(S_{m11} - r_{1d}\right)} \tag{2.32}$$

2.10.1 SOLT Calibration

A widely used calibration technique employs calibration standards of high precision. The most common such method is SOLT (short-open-load-thru) calibration, wherein a short circuit, an open circuit and a matched load are successively connected to one of the ports and measured on the VNA to accomplish the reflection calibration. After this, a thru standard is connected between ports 1 and 2, and transmission measurements carried out. Let us look in detail at the reflection calibration process.

Suppose our cal standards (denoted A, B and C) have $S_{A11} = -1$, $S_{B11} = +1$ and $S_{C11} = 0$ (it is not necessary for the cal standards to be ideal ones like this; the same general procedure will apply with somewhat more complicated equations to solve). Then we have the three equations

$$S_{mA11} = r_{1d} + t_1^2 \frac{-1}{1 + r_{1s}} \tag{2.33}$$

$$S_{mB11} = r_{1d} + t_1^2 \frac{1}{1 - r_{1s}} \tag{2.34}$$

$$S_{mC11} = r_{1d} \tag{2.35}$$

where S_{mA11}, S_{mB11} and S_{mC11} denote the raw measured values of S_{m11} at the ideal VNA with cal standards A, B or C connected to port 1, respectively. These equations are easily solved to give

$$t_1^2 = 2\frac{\left(S_{mA11} - S_{mC11}\right)\left(S_{mB11} - S_{mC11}\right)}{S_{mA11} - S_{mB11}} \tag{2.36}$$

$$r_{1s} = \frac{2S_{mC11} - S_{mA11} - S_{mB11}}{S_{mA11} - S_{mB11}} \tag{2.37}$$

$$\tau_{1d} = S_{mC11} \tag{2.38}$$

An exactly similar procedure applies to the determination of the S-parameters of error box E2 at port 2. Calculations related to the transmission calibration to determine Ex are analogous, though algebraically more complicated, and will not be presented here.

2.10.2 TRL Calibration

Calibration kits (sets of high precision cal standards) are expensive and are not always available for nonstandard or outdated types of transmission line. Fortunately, there are alternative calibration methods that do not require high precision cal standards and make only a modest sacrifice in accuracy. The most popular of these methods is TRL (thru-reflect-line), in which the "thru" standard is simply a direct connection between ports 1 and 2 (the connectors must be such as to permit this), the "reflect" standard is some load with a high reflection coefficient (its phase can be known only approximately) and the "line" standard is a length of transmission line whose electrical length is known very approximately (e. g., it is closer to $\lambda/4$ than to $3\lambda/4$). Similar algebra to that used for SOLT calibration shows that TRL calibration can not only determine the S-parameters of the error boxes, but also can determine precisely the reflection coefficient ρ_{cal} of the reflect standard and the transmission factor $e^{-\gamma l}$ of the line standard (see D. M. Pozar, *Microwave Engineering*, 3rd edition, pp. 193-196 for details).

At a frequency where the length of the line standard is at or near an integer number of half wavelengths, measurement of this cal standard will give the same values (or close to them) as measurement of the thru standard. Because of this, there are frequency limitations imposed on TRL calibrations that are not present in SOLT calibrations. As an example, if the thru standard has zero electrical length, and the length of the line standard in cm is l_{cm}, the largest contiguous frequency range in GHz that can be calibrated by the TRL method is

$$\frac{1.67}{l_{\text{cm}}\sqrt{\epsilon_e}} < f_{\text{GHz}} < \frac{13.33}{l_{\text{cm}}\sqrt{\epsilon_e}} \tag{2.39}$$

which is a maximum frequency ratio of 8:1 (there are also higher frequency ranges such as $\frac{16.67}{l_{\text{cm}}\sqrt{\epsilon_e}} < f_{\text{GHz}} < \frac{28.33}{l_{\text{cm}}\sqrt{\epsilon_e}}$, etc., but these have a much smaller relative bandwidth). Modern network analyzers have built-in capabilities for both SOLT and TRL calibrations, and often other calibration methods as well.

2.11 Practice questions

1. A measurement of a two-port gave the following S-matrix:

$$\mathbf{S} = \begin{bmatrix} 0.1\angle 0° & 0.8\angle 90° \\ 0.8\angle 90° & 0.2\angle 0° \end{bmatrix}$$

   Determine if the network is reciprocal and whether it is lossless.

2. In a common-source amplifier, define the S-parameters and relate them to quantities you have studied in circuit analysis.

3. What is the Smith chart? Which quantities can you plot on it?

4. What do concentric circles centered at the middle of the chart represent?

5. What do circles of constant resistance and those of constant reactance look like?

6. Which part of the chart corresponds to real impedances, and which to imaginary ones? Which part of the chart corresponds to capacitances, and which to inductances? What if you looked at the admittance instead of the impedance chart?

possible impedances. A practical difficulty in producing high-quality tuners is the fact that any realistic component will have loss, which will limit the impedance range. Namely, the very edge of the Smith chart is purely reactive and the presence of loss prevents a tuner from reaching those impedances. Air coaxial tuners have the lowest loss and are the most common. They typically consist of two movable parts with a different characteristic impedance as shown in Fig. 4.1, and are referred to as "slug tuners". Focus Microwaves, Inc. and Maury Microwave produce tuners capable of realizing VSWRs higher than 40:1 (see, e. g. http://www.focus-microwaves.com – look under manual and automatic tuners).

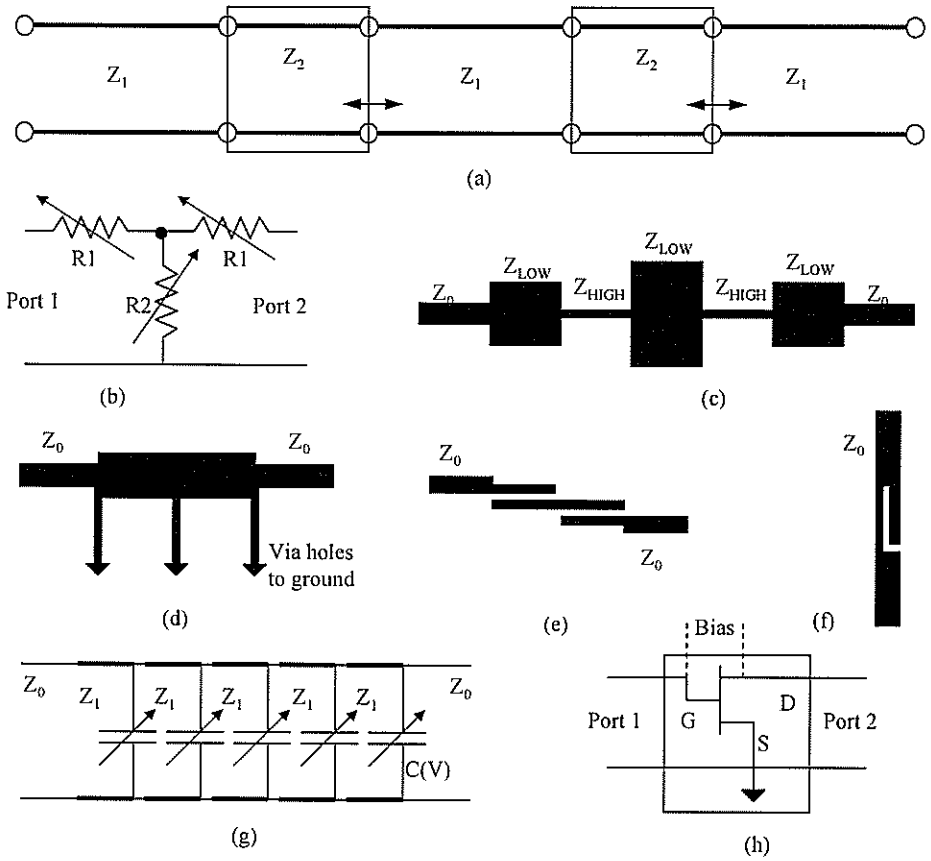

Figure 4.1: (a) Electrical model of a slug tuner. (b) Variable attenuator. (c) Low-pass filter implemented in microstrip, (d) Microstrip high-pass filter, (e) Microstrip coupled-line bandpass filter, (f) Microstrip band-stop filter, (g) Block diagram of a loaded-line phase shifter with varactor diodes, and (h) Two-port diagram of a common-source MESFET amplifier.

(3) *Attenuators* – are matched two-ports which absorb some power and are therefore lossy. They are reciprocal. Attenuators can be made to be variable, as shown in a lumped-element version, Fig. 4.1(b). They can also be implemented in waveguide using power transfer into non-propagating modes, as you will see in the lab. The loss is defined as the ratio of the output to input power, where the input power is the incident power minus the reflected power. This allows simple power calculations for cascaded two-port networks, and loss is really like (1/gain), or in dBs, negative

4.5 Operating Principles of the VNA

In section 2.10, we modeled a VNA by a hypothetical ideal VNA to which error boxes were connected to account for all the nonideal aspects of a real VNA. This allowed us to present the principles behind calibration of a VNA, but did not discuss how the ideal VNA could be realized, even approximately. As we saw in the previous chapter, the rapid variations with which the phase of a microwave signal is associated are virtually impossible for most instrumentation to follow accurately, and only time-average power (or amplitude) is directly measurable. In this section and the next one, we will show how such information can be used to accomplish the task of measuring ratios of wave amplitudes in RF and microwave networks.

The phase of a microwave signal can usually only be measured indirectly: for example, a reference signal and a signal to be measured can be sent to a mixer (see section 9.2) to obtain a lower-frequency signal related to the original, and the same thing repeated with the reference signal phase shifted by 90°. The powers of the two low-frequency outputs are then enough to determine the phase of the original signal. When combined with a power measurement to determine the amplitude of the signal, we have a measurement of the complex voltage (or current). Such an instrument is called a *vector voltmeter*. Note that the vector voltmeter is really a voltage comparator for two separate voltages—the one to be measured, and a reference voltage in the present example.

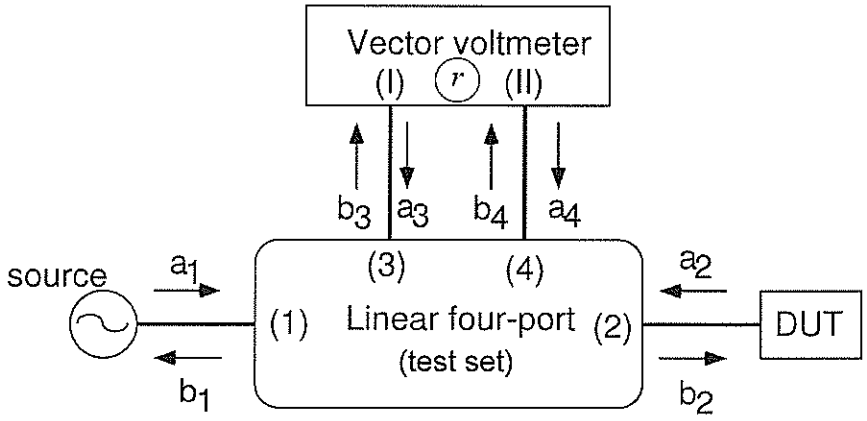

Figure 4.8: The vector voltmeter based network analyzer.

A common way to perform power measurements, which is used in most commercial instruments, is to combine a linear four-port (called a *test set*) with a vector voltmeter. The vector voltmeter used in commercial network analyzers is a two-port device that is linear with respect to the waves at its two RF ports (I and II). It generates a complex response that can be written in the form

$$r = K_0 + K_r \frac{a_I}{a_{II}} \tag{4.8}$$

where a_I and a_{II} are the incident wave amplitudes at its ports, and K_0 and K_r are complex constants characteristic of the vector voltmeter.

In a one-port reflection measurement, a vector voltmeter is connected to ports 3 and 4 of a test set. The other two ports are connected to a source and the device under test (DUT), Fig. 4.8. The configuration described here is usually called a *reflectometer*, and the test set typically consists of two directional couplers along with some auxiliary circuitry. The principle of operation of this circuit is as follows. We need to set up the equations for the wave amplitudes in the various ports, and establish the form of the relationships between them. The constants which appear in these relations will be

determined by calibration, in which known loads are connected at the DUT port, and the measured values of response from the vector voltmeter are used to obtain the constants.

The source sends a wave a_1 into port 1 of the test set, which we assume to be matched to the source. Parts of this wave reach the DUT and get reflected, and parts of it get to the ports of the vector voltmeter via ports 3 and 4 of the test set and get partially reflected there as well. The vector voltmeter samples different combinations of the waves that are incident and reflected at the DUT. Since the test set and the vector voltmeter are both linear multiports, we can write the outgoing waves from the test set in terms of a_1 and a_2 only:

$$\begin{aligned} b_2 &= M_1 a_1 + M_2 a_2 \\ b_3 &= L_1 a_1 + L_2 a_2 \\ b_4 &= K_1 a_1 + K_2 a_2 \end{aligned} \tag{4.9}$$

where the K's, M's and L's are complex constants that depend on the S-parameters of the test set and those of the vector voltmeter.

By definition, $a_2 = \rho b_2$, where ρ is the unknown reflection coefficient of the DUT, so we can solve for b_2 in terms of a_1 only, and b_3 and b_4 in terms of a_1 and b_2:

$$\begin{aligned} b_2 &= \frac{M_1}{1 - \rho M_2} a_1 \\ b_3 &= L_1 a_1 + L_2 \rho b_2 \\ b_4 &= K_1 a_1 + K_2 \rho b_2 \end{aligned} \tag{4.10}$$

From these formulas, the we can express the complex ratio b_3/b_4 in terms of the various network-analyzer-dependent constants (K_1, L_1, etc.), which left as an exercise. When you plug the result of your homework into this expression, and divide top and bottom by the coefficient of ρ in the numerator, you should get the following expression:

$$r = \frac{\rho + A}{B\rho + C}. \tag{4.11}$$

where A, B and C are complex constants dependent only on the properties of the network analyzer, and not on those of the DUT. So, the final result is that the value of r, which the vector voltmeter gives you, is a bilinear transform of the true reflection coefficient of the device you are measuring.

The result of the measurement is independent of the level of the test signal incident at port 1. The three unknown complex constants in (4.11) are dependent on the internal properties of the network analyzer, and can change due to component variations, changes in temperature and humidity, and so on. Thus, as we saw in section 2.10, three known cal standards can be measured to determine these constants. From the formula for r,

$$-A + \rho r B + r C = \rho. \tag{4.12}$$

which is a linear equation in the unknown constants A, B and C. Therefore, by observing the three values of r that result from measuring three known values of ρ, the constants A, B and C can be determined. Just as we saw from the error-box model in section 2.10, only three calibration standards are needed for a one-port measurement in this system.

The situation is a bit more complicated when the S-parameters of an unknown two-port are to be measured. The setup for doing this is shown in Fig. 4.9. The part of the test set connected to port 1 of the DUT is the reflectometer from above (it is in the dashed box in Fig. 4.9), and another port, the "transmission-return" receives the signal from port 2 of the DUT. A coaxial switch decides which signal is to be given to the vector voltmeter for the complex ratio measurement. To get the full S-matrix, the DUT must be flipped end for end once during the measurement, and the switch switched each time to observe the reflection at both ports and the transmission in both directions through the DUT. This gives a total of four measurements. A similar derivation as in the previous case of the reflection measurement

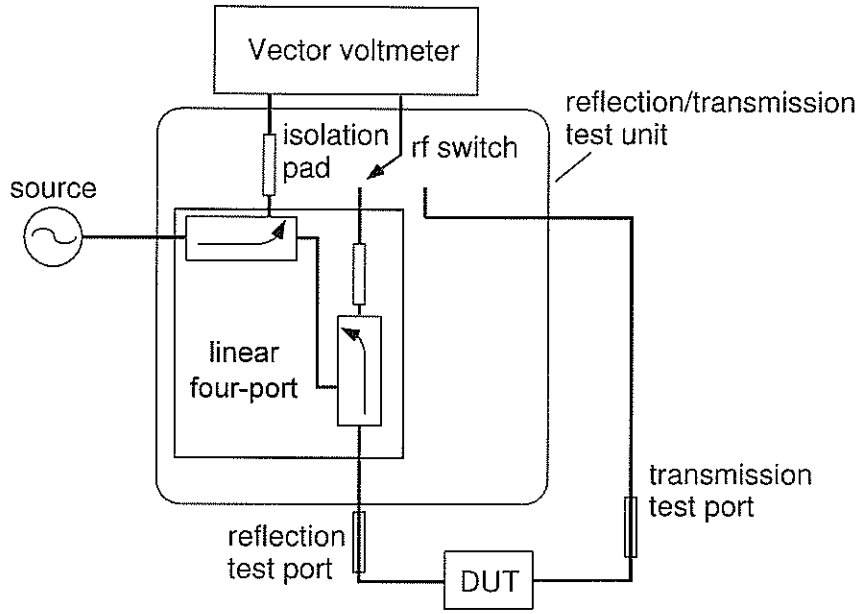

Figure 4.9: A reflection-transmission test set for full S-parameter measurements using a 4-port network analyzer.

can be derived, but the expressions for the S-parameters that come out of it are very messy. It turns out that you need to measure six known standards to perform a calibration. It is important to understand that in a network analyzer, these measurements are done at many frequencies (usually swept between a lower and upper limit), so you also need to measure your standards at all these frequencies of interest.

A full S-parameter test set, such as the ones used in the lab, consists of two transmission-reflection test sets like the one discussed above, placed back to back. Another coaxial switch selects which end of the setup receives the test signal. There is no need to flip the device, and this improves measurement speed and accuracy. The network analyzer contains a computer that does all the computations necessary to determine all the S-parameters, as well as many other parameters that you might be interested in.

In summary, four-port network analyzers measure the S-parameters of two-ports by using a single vector voltmeter with an arrangement of switches and directional couplers to route the appropriate signals to the voltmeter. The S-parameters of the measured two-port can be then found from the measured data after a bit of mathematical manipulation. If you wish to measure a 3-port or 4-port, typically all but two ports at a time are terminated in matched impedances and the 2-port measurements are repeated the necessary number of times. How many times do you need to repeat a two-port measurement to characterize a 4-port network?

4.6 Multiport Reflectometry

As we saw in section 4.5, the principle behind most commercial microwave VNAs is that of multiport reflectometry. There, we postulated the existence of a vector voltmeter without inquiring how such a device could be realized in practice. In this section we will discuss in detail another related modern method for reflection coefficient measurement that is also based on the use of interconnected multiports, but uses time-average power measurements directly rather than through the intermediary of a vector voltmeter. In the process, we will gain deeper insight into the various nonideal factors that are accounted

for by the calibration process.

Suppose that a microwave oscillator is connected to two directional couplers with fairly small coupling coefficients C_3 and C_4, and then to an unknown load whose reflection coefficient is ρ, as shown in Fig. 4.10. Power detectors, such as diode detectors, are connected to the coupled ports of the direc-

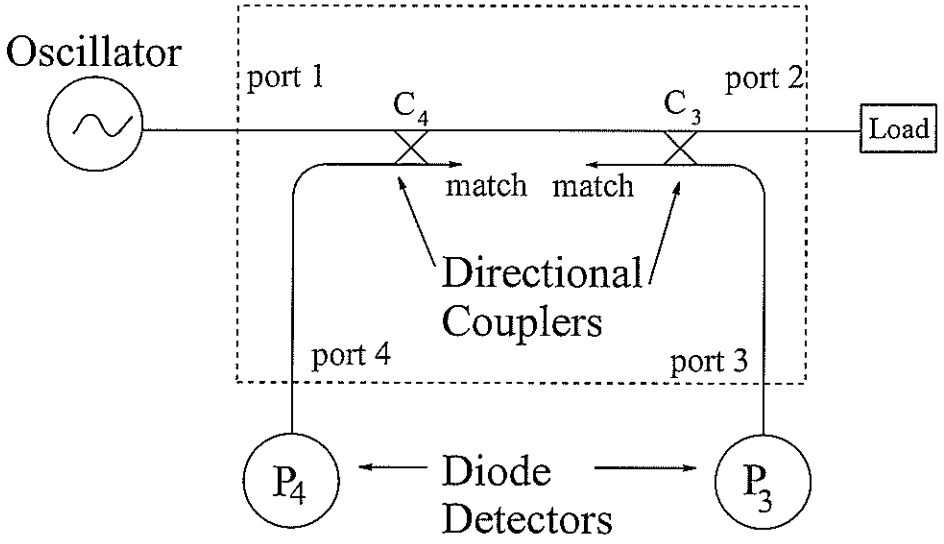

Figure 4.10: Four-port reflectometer (the test set is inside the dashed box).

tional couplers. The power detectors, oscillators and directional couplers will be assumed to have small reflection coefficients, so that $P_3 = |C_3|^2|a_1|^2$ and $P_4 = |C_4|^2|b_1|^2$. Under these conditions, the ratio of the measured powers will be

$$\frac{P_4}{P_3} = q_{43}|\rho|^2 \tag{4.13}$$

where $q_{43} = |C_4/C_3|^2$ is independent of the unknown reflection coefficient ρ. If diode detectors are used to measure power, (4.13) can be replaced by

$$\frac{V_4}{V_3} = Q_4|\rho|^2 \tag{4.14}$$

where V_3 and V_4 are the DC voltages measured at the diode (under zero bias voltage conditions). The constant Q_4 now depends on the properties of the directional couplers as well as those of the diodes, but still not on the unknown ρ; it is called a calibration constant and can be determined by a calibration procedure.

For the present case, it is sufficient to connect a short circuit calibration standard to the load port, for which we know that $\rho = -1$. Thus, the measurements of V_3 and V_4 would give:

$$Q_4 = \left.\frac{V_4}{V_3}\right|_{\rho=-1} \tag{4.15}$$

We do not need to have the directional couplers or diodes to be made to precise specifications, or even to be identical to each other. As long as the calibration measurement can be made, the constant Q_4 can be computed. Once this is done, the actual load can be connected to the load port, and the diode voltages measured. From (4.14), the magnitude of ρ can be determined.

Unfortunately, this procedure gives no information about the phase of ρ (we have made only a scalar network analyzer so far). To obtain phase information, we must modify the configuration of our reflectometer. Suppose now that we replace the circuit shown in Fig. 4.10 with the one shown in Fig. 4.11. Instead of a match, the fourth port of the second coupler is terminated in a short circuit whose

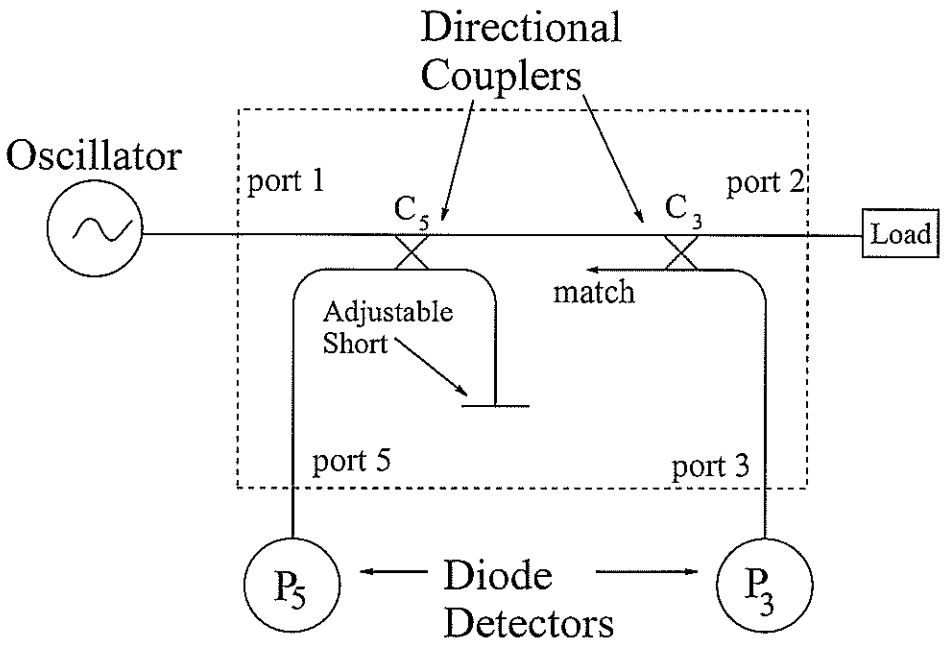

Figure 4.11: Modified four-port reflectometer.

position is adjustable. We rename the port where power is measured on this coupler to be port 5, to avoid confusion with the previous configuration. If the coupling coefficients of the directional couplers are again assumed to be small, then the ratio of the two diode voltages will have the form

$$\frac{V_5}{V_3} = Q_5|\rho - e^{j\phi_5}|^2 \tag{4.16}$$

where Q_5 and the angle ϕ_5 are calibration constants. The phase angle ϕ_5 is dependent on the path length difference between a_1 and b_1 due to the routes they travel on the main line and on the coupled line. All that really matters is that all calibration constants are independent of the load reflection coefficient, and can be determined by calibration measurements (the details of which we will postpone until a little later).

To simplify our equations somewhat, we introduce the notation

$$\Lambda_n = \frac{V_n}{V_3}; \qquad n = 4, 5, \ldots \tag{4.17}$$

for ratios of measured voltages (these are real and ≥ 0). If the calibration constants Q_5 and ϕ_5 are known, then (4.16) says that the unknown ρ lies on a circle in the complex plane, centered at $\rho_5 = e^{j\phi_5}$ and having a radius

$$\sqrt{\frac{\Lambda_5}{Q_5}} \equiv R_5 \tag{4.18}$$

If this information is combined with that from (4.14), which says that ρ lies on a circle centered at the origin with a radius

$$\sqrt{\frac{\Lambda_4}{Q_4}} \equiv R_4 \tag{4.19}$$

we conclude that ρ must be located at one of the intersection points of these two circles. To resolve the question of which intersection is the correct one, we must take a further measurement, replacing the circuit of Fig. 4.11 with a similar one, wherein the short circuit is adjusted so as to give a different phase angle ϕ_6. Since the diode and directional coupler properties may also be different, we have

$$\Lambda_6 = Q_6|\rho - e^{j\phi_6}|^2 \tag{4.20}$$

meaning that ρ is located on yet a third circle, centered at $\rho_6 = e^{j\phi_6}$ and with a radius

$$\sqrt{\frac{\Lambda_6}{Q_6}} \equiv R_6 \tag{4.21}$$

The intersection of the three circles thus determines both the magnitude and phase of ρ uniquely, as shown in Fig. 4.12.

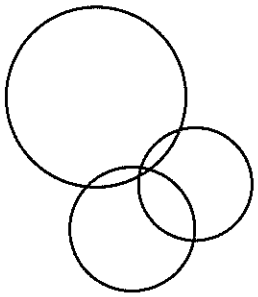

Figure 4.12: Intersection of three circles to determine complex ρ.

We do not need to use three different experimental configurations to make our measurements. All three can be combined into one circuit, as shown in Fig. 4.13. If this is done, there can arise significant

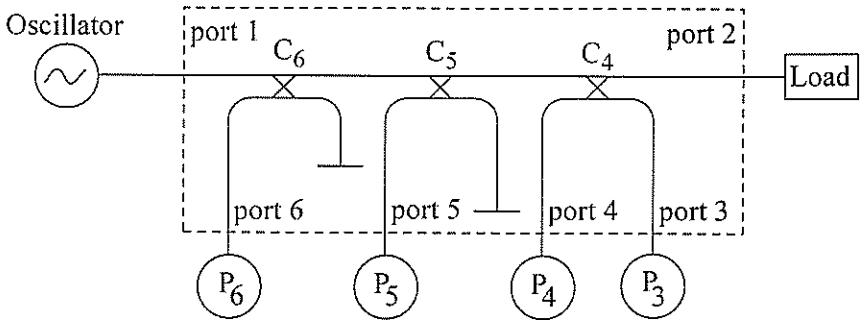

Figure 4.13: Six-port reflectometer.

deviations from the assumptions we made in deriving our equations. For example, the directional couplers can reintroduce some of the sampled waves back into the main line, thus modifying what we are trying

to measure. For this reason, we have to modify the equations (4.14) (4.16) and (4.20) to allow the centers of these circles in the complex ρ-plane to be at arbitrary locations ρ_4, ρ_5 and ρ_6, so that for the reflectometer in Fig. 4.13 they take the form

$$|\rho - \rho_n|^2 = \frac{A_n}{Q_n} = R_n^2; \qquad n = 4, 5, 6 \tag{4.22}$$

for some positive real calibration constants Q_4, Q_5 and Q_6, and some complex calibration constants ρ_4, ρ_5 and ρ_6, all independent of the load reflection coefficient ρ.

If the calibration constants in (4.22) are known, we have three real equations for two real unknowns (the real and imaginary parts of $\rho = u + jv$). Experimental error will always result in the three circles not intersecting exactly, but merely coming close to doing so. The extent to which they do not all intersect at the same point is one measure of the error in determining the reflection coefficient. Indeed, drawing the three circles on a graph (a Smith chart will do nicely, but is not necessary) and locating their near intersection point is one way to compute ρ from the measured data. This process can be automated using an optimization technique such as "least squares" solution of (4.22). However, the determination of ρ in this way is somewhat arbitrary, since the choice of error criterion that gives a "best fit" solution of (4.22) can be made in many different ways. A more systematic approach is to find the *radical center* of the three circles, as we will now describe. Once this is done it is a good idea to substitute the calculated value of ρ back into the original equations to check that a good solution has indeed been found, and to estimate the experimental error.

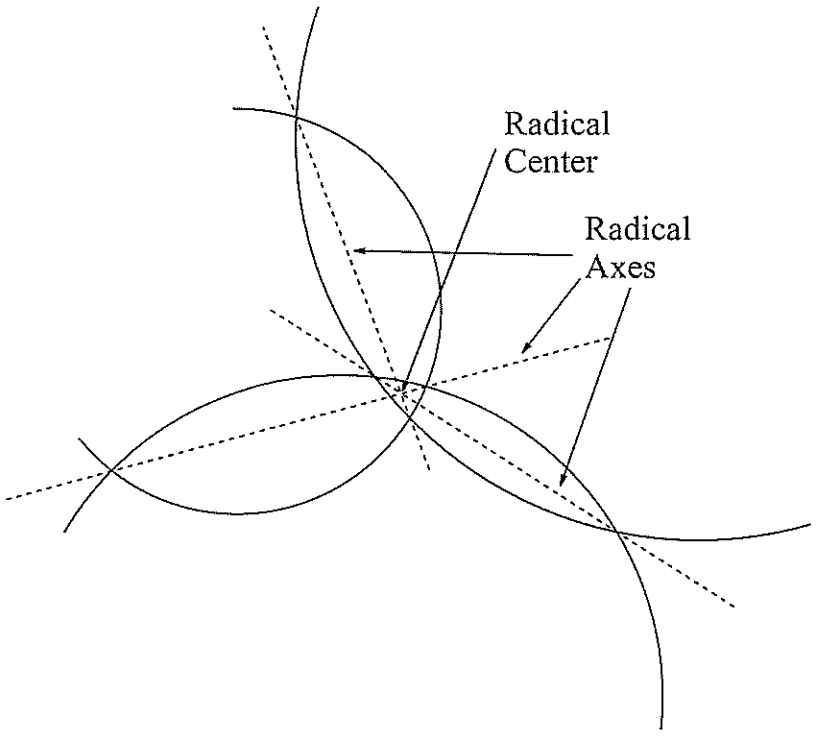

Figure 4.14: Radical axes and radical center of three circles in the complex ρ-plane.

If we take a closer look at the near intersection of the three circles, we have the situation shown in Fig. 4.14. A straight line drawn through the intersection points of any pair of circles is called the *radical*

axis of that pair of circles. A theorem of geometry tells us that the three radical axes generated by our three circles must all intersect in a single point, if the centers ρ_4, ρ_5 and ρ_6 of the circles are all different. This point is called the radical center of the three circles, and from Fig. 4.14 we can see that it is in a certain sense the best fit solution of equations (4.22). It can be calculated by first deriving the equation for a typical radical axis, say the one for the circles centered at ρ_4 and ρ_5. We have

$$(u-u_4)^2+(v-v_4)^2=R_4^2; \qquad (u-u_5)^2+(v-v_5)^2=R_5^2 \tag{4.23}$$

Subtracting these two equations and rearranging gives an equation for the radical axis:

$$u(u_4-u_5)+v(v_4-v_5)=K_4-K_5 \tag{4.24}$$

where

$$K_n=\frac{u_n^2+v_n^2-R_n^2}{2}=\frac{|\rho_n|^2-R_n^2}{2}; \qquad n=4,5,6 \tag{4.25}$$

In a similar way, the equation for the radical axis of the circles centered at ρ_5 and ρ_6 is

$$u(u_5-u_6)+v(v_5-v_6)=K_5-K_6 \tag{4.26}$$

and the radical center is found by solving (4.24) and (4.26) using determinants:

$$\boxed{u=\frac{N_u}{D}; \qquad v=\frac{N_v}{D}} \tag{4.27}$$

where N_u, N_v and D are the matrix determinants

$$N_u=\det\begin{bmatrix}(K_4-K_5) & (v_4-v_5)\\ (K_5-K_6) & (v_5-v_6)\end{bmatrix} \qquad N_v=\det\begin{bmatrix}(u_4-u_5) & (K_4-K_5)\\ (u_5-u_6) & (K_5-K_6)\end{bmatrix} \tag{4.28}$$

and

$$D=\det\begin{bmatrix}(u_4-u_5) & (v_4-v_5)\\ (u_5-u_6) & (v_5-v_6)\end{bmatrix} \tag{4.29}$$

Equation (4.27) is ready to use once the calibration constants are found: u_n, v_n and Q_n are known from calibration, and Λ_n (and therefore R_n and K_n) are known from measurement. The resulting value of $\rho=u+jv$ should be substituted back into (4.22) to check the accuracy of the solution.

The calibration constants have to be determined by a calibration procedure, just as with any network analyzer. Because there are more calibration constants to determine than when we assumed $\rho_4=0$ and that ρ_5 and ρ_6 lie on the unit circle, more calibration measurements and calculations will have to be done than in that case, but the resulting value found for an unknown ρ will be more accurate. Because there are three real quantities (one real Q_n and one complex ρ_n) for each n to be determined in (4.22), it would seem that three calibration standards will have to be measured, giving three conditions to be satisfied for Q_n and ρ_n for each $n=4,5,6$. However, we encounter a situation similar to the one above when finding the unknown load reflection coefficient ρ, in that three cal standards will give two possible solutions for the calibration constants, and an extra cal standard is needed to resolve this ambiguity.

Let our first three cal standards have known values of reflection coefficient $\rho_a=u_a+jv_a$, $\rho_b=u_b+jv_b$ and $\rho_c=u_c+jv_c$ (chosen in some convenient way), and let the final cal standard be a matched load ($\rho_d=0$). If we denote the corresponding measured values of Λ_n (for each $n=4,5,6$) by Λ_{na}, Λ_{nb}, Λ_{nc} and Λ_{nd}, then at each port n, (4.22) gives four separate equations

$$|\rho_a-\rho_n|^2=\frac{\Lambda_{na}}{Q_n}; \qquad n=4,5,6 \tag{4.30}$$

$$|\rho_b-\rho_n|^2=\frac{\Lambda_{nb}}{Q_n}; \qquad n=4,5,6 \tag{4.31}$$

$$|\rho_c - \rho_n|^2 = \frac{\Lambda_{nc}}{Q_n}; \qquad n = 4,5,6 \tag{4.32}$$

$$|\rho_n|^2 = \frac{\Lambda_{nd}}{Q_n}; \qquad n = 4,5,6 \tag{4.33}$$

for determining Q_n and ρ_n, subject to the additional constraint that $Q_n > 0$. We can temporarily eliminate Q_n from these equations by dividing each of (4.30)-(4.32) by (4.33), giving:

$$|\rho_a - \rho_n|^2 = \frac{\Lambda_{na}}{\Lambda_{nd}} |\rho_n|^2; \qquad n = 4,5,6 \tag{4.34}$$

$$|\rho_b - \rho_n|^2 = \frac{\Lambda_{nb}}{\Lambda_{nd}} |\rho_n|^2; \qquad n = 4,5,6 \tag{4.35}$$

$$|\rho_c - \rho_n|^2 = \frac{\Lambda_{nc}}{\Lambda_{nd}} |\rho_n|^2; \qquad n = 4,5,6 \tag{4.36}$$

Some algebra will show that (4.34)-(4.36) can be rewritten as

$$\left|\rho_n - \frac{\Lambda_{nd}}{\Lambda_{nd} - \Lambda_{na}}\rho_a\right|^2 = \frac{\Lambda_{na}\Lambda_{nd}}{(\Lambda_{nd} - \Lambda_{na})^2} |\rho_a|^2; \qquad n = 4,5,6 \tag{4.37}$$

$$\left|\rho_n - \frac{\Lambda_{nd}}{\Lambda_{nd} - \Lambda_{nb}}\rho_b\right|^2 = \frac{\Lambda_{nb}\Lambda_{nd}}{(\Lambda_{nd} - \Lambda_{nb})^2} |\rho_b|^2; \qquad n = 4,5,6 \tag{4.38}$$

$$\left|\rho_n - \frac{\Lambda_{nd}}{\Lambda_{nd} - \Lambda_{nc}}\rho_c\right|^2 = \frac{\Lambda_{nc}\Lambda_{nd}}{(\Lambda_{nd} - \Lambda_{nc})^2} |\rho_c|^2; \qquad n = 4,5,6 \tag{4.39}$$

It will be seen that these equations are circles in the complex ρ_n-plane in the same form as (4.22), although now the unknown is ρ_n, while ρ_a, ρ_b, ρ_c, Λ_{na}, Λ_{nb}, Λ_{nc} and Λ_{nd} are known.

We may thus use the same method as before to find the ρ_n. After some algebra we arrive at

$$\boxed{u_n = \frac{N_{un}}{D_n}; \qquad v_n = \frac{N_{vn}}{D_n}} \tag{4.40}$$

where N_{un}, N_{vn} and D_n are the matrix determinants

$$N_{un} = \frac{1}{2}\det\begin{bmatrix} \left(\frac{|\rho_a|^2}{\Lambda_{nd} - \Lambda_{na}} - \frac{|\rho_b|^2}{\Lambda_{nd} - \Lambda_{nb}}\right) & \left(\frac{v_a}{\Lambda_{nd} - \Lambda_{na}} - \frac{v_b}{\Lambda_{nd} - \Lambda_{nb}}\right) \\ \left(\frac{|\rho_b|^2}{\Lambda_{nd} - \Lambda_{nb}} - \frac{|\rho_c|^2}{\Lambda_{nd} - \Lambda_{nc}}\right) & \left(\frac{v_b}{\Lambda_{nd} - \Lambda_{nb}} - \frac{v_c}{\Lambda_{nd} - \Lambda_{nc}}\right) \end{bmatrix} \tag{4.41}$$

$$N_{vn} = \frac{1}{2}\det\begin{bmatrix} \left(\frac{u_a}{\Lambda_{nd} - \Lambda_{na}} - \frac{u_b}{\Lambda_{nd} - \Lambda_{nb}}\right) & \left(\frac{|\rho_a|^2}{\Lambda_{nd} - \Lambda_{na}} - \frac{|\rho_b|^2}{\Lambda_{nd} - \Lambda_{nb}}\right) \\ \left(\frac{u_b}{\Lambda_{nd} - \Lambda_{nb}} - \frac{u_c}{\Lambda_{nd} - \Lambda_{nc}}\right) & \left(\frac{|\rho_b|^2}{\Lambda_{nd} - \Lambda_{nb}} - \frac{|\rho_c|^2}{\Lambda_{nd} - \Lambda_{nc}}\right) \end{bmatrix} \tag{4.42}$$

and

$$D_n = \det\begin{bmatrix} \left(\frac{u_a}{\Lambda_{nd} - \Lambda_{na}} - \frac{u_b}{\Lambda_{nd} - \Lambda_{nb}}\right) & \left(\frac{v_a}{\Lambda_{nd} - \Lambda_{na}} - \frac{v_b}{\Lambda_{nd} - \Lambda_{nb}}\right) \\ \left(\frac{u_b}{\Lambda_{nd} - \Lambda_{nb}} - \frac{u_c}{\Lambda_{nd} - \Lambda_{nc}}\right) & \left(\frac{v_b}{\Lambda_{nd} - \Lambda_{nb}} - \frac{v_c}{\Lambda_{nd} - \Lambda_{nc}}\right) \end{bmatrix} \tag{4.43}$$

With $\rho_n = u_n + jv_n$ now determined, we obtain Q_n from (4.33):

$$\boxed{Q_n = \frac{\Lambda_{nd}}{|\rho_n|^2}} \tag{4.44}$$

Once again, it is important to verify that the original equations (4.30)-(4.32) are accurately satisfied once the computation of the calibration constants has been completed. It may be necessary to adjust the positions of the sliding shorts in the six-port network in order to be able to obtain a more accurate calibration.

To summarize, we must first perform calibration measurements and use equations (4.40) and (4.44) to evaluate the calibration constants. Then the DUT is connected and measured, from which we determine the real and imaginary parts of the unknown ρ using (4.27).

4.7 Practice questions

1. Show that a four port network can satisfy the matched, reciprocal and lossless conditions simultaneously.

2. Show that the ideal isolator is lossy.

3. Show that the ideal phase shifter is lossless.

4. Write down the scattering matrix of an ideal lumped element low-pass filter in the (a) pass band and (b) stop band. Repeat for a transmission-line low-pass filter such as in Fig. 4.1(c).

5. Write down the scattering matrix for a 3-dB directional coupler for which the two non-isolated outputs are in phase quadrature.

6. How does odd and even mode decomposition work? What kind of a network do you have to have in order to be allowed to use odd and even mode decomposition?

7. Sketch the odd and even mode circuits of a microstrip branch line coupler.

8. Sketch the odd and even mode circuits of a Wilkinson power divider, shown in Figure 4.2(d).

9. What are the impedances of $\lambda/8$-long short and opened stubs of characteristic impedance Z_0?

10. Apply results from question #10 to calculating the odd and even mode reflection and transmission coefficients for the branch line directional coupler $(\rho_o, \rho_e, \tau_o, \tau_e)$.

11. If you had a 20-dB directional coupler, how could you use it to measure a reflection coefficient?

12. Sketch the four-port reflectometer part of a network analyzer. Why do you need the linear 4-port?

13. Write down the calibration procedure (find the constants A, B and C) for a short-open-load calibration. How would you do a calibration if you only had one of the standards, say the short?

14. The network analyzer has 2 coaxial cables coming out of it. These are two ports. How would you measure the parameters of a three-port circuit using the network analyzer? How would you fully characterize a four-port device using a two-port network analyzer?

15. For three mutually intersecting circles as shown in Fig. 4.14, each pair of circles intersects at two points. Show that if the three radical axes are not parallel to each other, they intersect at a single point, which can be used as a best fit to the equations described by the three circles.